SARS-CoV-2 Uses CD4 to Infect T Helper Lymphocytes

Gustavo G. Davanzo[1,26], Ana C. Codo[1,26], Natalia S. Brunetti[2,26] , Vinícius Boldrini[2,26] , Thiago L. Knittel[3,26], Lauar B. Monterio[1,26], Diogo de Moraes[4,26], Allan J. R. Ferrari[5,26], Gabriela F. de Souza[6,26], Stefanie P. Muraro[6,26], Gerson S. Profeta[3,27], Natália S. Wassano[7,27], Luana N. Santos[8,27], Victor C. Carregari[9,27], Arthur H. S. Dias[5,27], João Victor Virgilio-da-Silva[1,27], Ícaro Castro[10], Lícia C. Silva-Costa[9], Andre Palma[12], Eli Mansour[12], Raisa G. Ulaf[12], Ana F. Bernardes[12], Thyago A. Nunes[12], Luciana C. Ribeiro[12], Marcus V. Agrela[12], Maria Luiza Moretti[12], Lucas I. Buscaratti[8], Fernanda Crunfli[9], Raissa G. Ludwig[3], Jaqueline A. Gerhardt[7], Renata Seste-Costa[2], Julia Forato[6], Mariene R. Amorin[6], Daniel A. T. Texeira[6], Pierina L. Parise[6], Matheus C. Martini[6], Karina Bispo-dos-Santos[6], Camila L. Simeoni[6], Fabiana Granja[6], Virginia C. Silvestrini[13], Eduardo B. de Oliveira[13], Vitor M. Faça[13], Murilo Carvalho[14,15], Bianca G. Castelucci[14,15], Alexandre B. Pereira[14], Laís D. Coimbra[14], Patricia B. Rodrigues[16], Arilson Bernardo S. P. Gomes[16], Fabrício B. Pereira[17], Leonilda M. B. Santos[18,19], Andrei C. Sposito[20], Robson F. Carvalho[4], Andre S. Vieira[21], Marco A. R. Vinolo[16,22,23], André Damasio[7,22], Licio A. Velloso[12,23], Helder I. Nakaya[10], Henrique Marques-Souza[7,8], Rafael E. Marques[14], Daniel Martins-de-Souza[9,22,24,25], Munir S. Skaf[5], José Luiz Proença-Modena[6,22], Pedro M. Moraes-Vieira[1,22,23], Marcelo A. Mori[3,22,23,*], Alessandro S. Farias[2,19,22,23,*]

[1]Laboratory of Immunometabolism, Department of Genetics, Microbiology and Immunology, Institute of Biology, University of Campinas (UNICAMP), Campinas, Brazil;

[2]Autoimmune Research Laboratory, Department of Genetics, Microbiology and Immunology, Institute of Biology, University of Campinas (UNICAMP), Campinas, Brazil;

[3]Laboratory of Aging Biology, Department of Biochemistry and Tissue Biology, Institute of Biology, University of Campinas (UNICAMP), Campinas, Brazil;

[4]Department of Structural and Functional Biology, Institute of Biosciences, Sao Paulo State University (UNESP), Botucatu, Brazil;

[5]Institute of Chemistry and Center for Computing in Engineering and Sciences, University of Campinas, Campinas (UNICAMP), Campinas, Brazil;

[6]Laboratory of Emerging Viruses, Department of Genetics, Microbiology and Immunology, Institute of Biology, University of Campinas (UNICAMP), Campinas, Brazil;

[7]Department of Biochemistry and Tissue Biology, Institute of Biology, University of Campinas (UNICAMP), Campinas, Brazil;

[8]Brazilian Laboratory on Silencing Technologies (BLaST), Department of Biochemistry and Tissue Biology, Institute of Biology, University of Campinas (UNICAMP), Campinas, Brazil;

[9]Laboratory of Neuroproteomics, Department of Biochemistry and Tissue Biology, Institute of Biology, University of Campinas (UNICAMP), Campinas, Brazil;

[10]Department of Clinical and Toxicological Analyses, School of Pharmaceutical Sciences, University of São Paulo, São Paulo, Brazil;

[12]Department of Internal Medicine, School of Medical Sciences, University of Campinas (UNICAMP), Campinas, Brazil;

[13]Department of Biochemistry and Immunology, Ribeirão Preto Medical School, University of São Paulo; Ribeirão Preto, Brazil;

[14]National Biosciences Laboratory (LNBio), Brazilian Center for Research in Energy and Materials (CNPEM), Campinas, Brazil;

[15]Brazilian Synchrotron Light Laboratory (LNLS), Brazilian Center for Research in Energy and Materials (CNPEM), Campinas, Brazil;

[16]Laboratory of Immunoinflammation, Department of Genetics, Microbiology and Immunology, Institute of Biology, University of Campinas (UNICAMP), Campinas, Brazil;

[17]Hematology and hemotherapy Center, University of Campinas (UNICAMP), Campinas, Brazil;

[18]Neuroimmunology Unit, Department of Genetics, Microbiology and Immunology, University of Campinas (UNICAMP), Campinas, Brazil;

[19]National Institute of Science and Technology on Neuroimmunomodulation (INCT-NIM) – Oswaldo Cruz Institute, Oswaldo Cruz Foundation, Rio de Janeiro, Brazil;

[20]Laboratory of Vascular Biology and Arteriosclerosis, School of Medical Sciences, University of Campinas (UNICAMP), Campinas, Brazil;

[21]Laboratory of Electrophysiology, Neurobiology and Behavior, University of Campinas (UNICAMP), Campinas, Brazil;

[22]Experimental Medicine Research Cluster (EMRC), University of Campinas (UNICAMP), Campinas, Brazil;

[23]Obesity and Comorbidities Research Center (OCRC), University of Campinas (UNICAMP), Campinas, Brazil;

[24]D'Or Institute for Research and Education (IDOR), São Paulo, Brazil;

[25]National Institute of Science and Technology in Biomarkers for Neuropsychiatry (INCT-INBION), São Paulo, Brazil.

[26]These authors contributed equally to this work

[27]These authors contributed equally to this work

*Corresponding Authors and Lead Contacts: asfarias@unicamp.br (A.S.F.) or morima@unicamp.br (M.A.M.).

Abstract

The severe acute respiratory syndrome coronavirus 2 (SARS-CoV-2) is the agent of a major global outbreak of respiratory tract disease known as coronavirus disease-2019 (COVID-19). SARS-CoV-2 infects the lungs and may cause several immune-related complications such as lymphocytopenia and cytokine storm which are associated with the severity of the disease and predict mortality[1,2]. The mechanism by which SARS-CoV-2 infection may result in immune system dysfunction is not fully understood. Here we show that SARS-CoV-2 infects human $CD4^+$ T helper cells, but not $CD8^+$ T cells, and is present in blood and bronchoalveolar lavage T helper cells of severe COVID-19 patients. We demonstrated that SARS-CoV-2 spike glycoprotein (S) directly binds to the CD4 molecule, which in turn mediates the entry of SARS-CoV-2 in T helper cells in a mechanism that also requires ACE2 and TMPRSS2. Once inside T helper cells, SARS-CoV-2 assembles viral factories, impairs cell function and may cause cell death. SARS-CoV-2 infected T helper cells express higher amounts of IL-10, which is associated with viral persistence and disease severity. Thus, CD4-mediated SARS-CoV-2 infection of T helper cells may explain the poor adaptive immune response of many COVID-19 patients.

Main

Coronavirus disease 2019 (COVID-19), which is caused by the severe acute respiratory syndrome coronavirus 2 (SARS-CoV-2), has emerge in Wuhan in December of 2019. COVID-19 rapidly spread across the globe[3,4], being declared a pandemic by the WHO in March 11th. COVID-19 has caused nearly one million deaths around the world as of September 20th, 2020. Most of the deaths are associated with acute pneumonia, cardiovascular complications, and organ failure due to hypoxia, exacerbated inflammatory responses and widespread cell death[1,5]. Individuals that progress to the severe stages of COVID-19 manifest marked alterations in the immune response characterized by reduced overall protein synthesis, cytokine storm, lymphocytopenia and T cell exhaustion[6-8]. In addition to these acute effects on the immune system, most convalescent individuals present low titres of neutralizing antibodies[9]. Moreover, the levels of antibodies against SARS-CoV-2 decay rapidly after recovery[10], suggesting that SARS-CoV-2 infection may exert profound and long-lasting complications to adaptive immunity. In this context, one question that remains to be answered is how SARS-CoV-2 exert these effects on the immune system.

To infect cells, the spike glycoprotein of SARS-CoV-2 (sCoV-2) binds to the host angiotensin-converting enzyme 2 (ACE2), after which it is then cleaved by TMPRSS2 [11]. While TMPRSS2 is ubiquitously expressed in human tissues (**fig. S1**), ACE2 is mainly expressed in epithelial

and endothelial cells, as well as in the kidney, testis and small intestine (**fig. S1**). Still, a wide variety of cell types are infected by SARS-CoV-2[12-14], even though some of these cells express very low levels of ACE2. We showed that this is the case for lymphocytes (**fig. S2**). This finding suggests that SARS-CoV-2 has either an alternative mechanism to enter the cells or that auxiliary molecules at the plasma membrane may fix the virus until it interacts with an ACE2 molecule.

Since the structures of the spike of SARS-CoV-1 (sCoV-1) and the sCoV-2 proteins are similar[15,16], we used the P-HIPSTer algorithm to uncover human proteins that putatively interact with the viruses[17]. Seventy-one human proteins were predicted to interact with sCoV-1 (**fig. S3**). We then cross-referenced the proteins with five databases of plasma membrane proteins to identify the ones located on the cell surface (**see Methods for details**). CD4 was the only protein predicted to interact with sCoV-1 that appeared in all five databases (**fig. S3**). CD4 is expressed mainly in T helper lymphocytes and has been shown to be the gateway for HIV[18]. Since $CD4^+$ T lymphocytes orchestrate innate and adaptive immune responses[19,20], infection of $CD4^+$ T cells by SARS-CoV-2 might explain lymphocytopenia and dysregulated inflammatory response in severe COVID-19 patients. Moreover, from an evolutionary perspective, the infection of $CD4^+$ T cells represents an effective mechanism for viruses to escape the immune response[21].

To test whether human primary T cells are infected by SARS-CoV-2, we purified $CD3^+CD4^+$ and $CD3^+CD8^+$ T cells from the peripheral blood of non-infected healthy controls/donors (HC), incubated these cells with SARS-CoV-2 for 1h, and then exhaustively washed them to remove any residual virus. The viral load was measured 24h post-infection. We were able to detect SARS-CoV-2 RNA in primary $CD4^+$ T cells but not $CD8^+$ T cells (**fig. 1A**). To confirm the presence of SARS-CoV-2 infection, we performed *in situ* hybridization using probes against the viral RNA-dependent RNA polymerase (RdRp) gene, immunofluorescence for sCoV-2 and transmission electron microscopy. All three approaches confirmed that SARS-CoV-2 infects $CD4^+$ T cells (**fig. 1B, 1C and fig. S4**). Moreover, we detected different SARS-CoV-2 RNAs in infected $CD4^+$ T cells (**fig. S5A**). Notably, the viral RNA level increases with time (**fig. 1D**) and we identified the presence of the negative strand (antisense) of SARS-CoV-2 in the infected cells (**fig. 1E**), demonstrating that the virus is able to assemble viral factories and replicate in T helper cells. Plaque assay also revealed that SARS-CoV-2-infected $CD4^+$ T cells produce infectious viral particles (**fig. 1F and S5B-C**).

To confirm that SARS-CoV-2 infects $CD4^+$ T cells *in vivo*, we purified $CD4^+$ and $CD8^+$ T cells from peripheral blood cells of COVID-19 patients (**table S1**). Similar to our *ex vivo* findings, SARS-CoV-2 RNA was detected in $CD4^+$ T cells, but not in $CD8^+$ T cells from COVID-19

patients (**fig. 1G**). Yet, the viral load was markedly higher in $CD4^+$ T cells from severe COVID-19 patients in comparison to patients with the moderate form of the disease (**fig. 1G**). Using publicly available single-cell sequencing data[22], we were also able to detect the presence of SARS-CoV-2 RNA in 2.1% of $CD4^+$ T cells of the bronchoalveolar lavage (BAL) of patients with the severe but not the moderate form of COVID-19 (**fig. 1H**). Thus, our data demonstrate that SARS-CoV-2 infects $CD4^+$ T cells and the infection associates with the severity of COVID-19.

We sought to explore the role of the CD4 molecule in SARS-CoV-2 infection. Based on the putative interaction found using P-HIPSTer, we performed molecular docking analyses and predicted that sCoV-2 receptor binding domain (RBD) directly interacts with the N-terminal domain (NTD) of CD4 Ig-like V type (**fig. 2A and S6**). Molecular dynamics simulations with stepwise temperature increase were applied to challenge the kinetic stability of the docking model representatives (**fig. 2B**). Two models remained stable after the third step of simulation at 353 Kelvin and represent likely candidates for the interaction between the CD4 NTD and sCoV-2 RBD (**fig. 2B**). Additionally, convergence towards the two surviving models was tested for closely related binding mode models present among the remaining cluster candidates and was verified in one case, which indicates plausible and rather stable interaction between CD4 NTD and sCoV-2 RBD (**fig. S6**). The interaction region of RBD is predicted to overlap with that of human ACE2 (**fig. 2C and 2D**). The interaction region of RBD is predicted to overlap with that of human ACE2 **(fig. 2C and 2D**). The interaction between CD4 and sCoV-2 was confirmed by co-immunoprecipitation of sCoV-2 and full length recombinant CD4 (**fig. 3A**). Consistent with a mechanism where CD4-sCoV-2 interaction is required for infection, we observed that increasing concentrations of soluble CD4 (sCD4) reduced CD4+ T cell infection by SARS-CoV-2 (**fig. 3B**).

To gain further insights into the importance of CD4-sCoV-2 binding to SARS-CoV-2 infection, we purified $CD4^+$ T cells and pre-treated them with anti-CD4 polyclonal antibody. We observed a dose-dependent reduction in viral load in $CD4^+$ T cells pre-treated with anti-CD4 antibody, showing that CD4 is necessary for SARS-CoV-2 infection (**fig. 3C**). Remarkably, the same monoclonal antibody that has been used to block HIV entry in $CD4^+$ T cells [18,23] also blocked SARS-CoV-2 entry in a dose dependent manner (**fig. 3D**). This observation is consistent with our *in silico* model (**fig. 2 and S6E**) that predicts that sCoV-2 binds to a region of CD4 which is neighbor to where envelope-displayed glycoprotein spike complex (Env) is shown to bind [24]. These data demonstrate that the CD4 molecule is necessary for infection of $CD4^+$ T cells by SARS-CoV-2 and suggest that SARS-CoV-2 may use a mechanism that somehow resembles HIV infection.

In HIV infection, CD4 alone is not sufficient to allow the virus to enter $CD4^+$ T cells[25]. Instead, the Env must also interact with co-receptors (CCR5 or CXCR4)[25,26]. In this context, we tested whether CD4 alone was sufficient to allow SARS-CoV-2 entry. Inhibition of ACE2 using polyclonal antibody abrogated SARS-CoV-2 entry in $CD4^+$ T cells (**fig. 3E**), suggesting that the canonical entry mechanism involving ACE2 and TMPRSS2[11] is also required. To exclude the possibility that the polyclonal anti-ACE2 antibody cross-reacts with CD4, we designed a peptide to specifically block ACE2-sCoV-2 interaction (**fig. S7**). The peptide recapitulated the effect of anti-ACE2 antibody and also reduced the viral load in a dose dependent manner (**fig. 3F**). Similarly, inhibition of TMPRSS2 with camostat mesylate also reduced SARS-CoV-2 infection (**fig. 3G**). Hence, ACE2, TMPRSS2 and CD4 act in concert to allow the infection of $CD4^+$ T cells by SARS-CoV-2.

To assess the consequences of SARS-CoV-2 infecting $CD4^+$ T cells, we performed mass spectrometry-based shotgun proteomics in *ex vivo* infected $CD4^+$ T cells. We found that SARS-CoV-2 infection affects multiple housekeeping pathways associated with the immune system, infectious diseases, cell cycle and cellular metabolism (**fig. 4A, 4B, S8, and S9**), similarly to what was observed in HIV-infected $CD4^+$ T cells [27]. SARS-CoV-2 infection elicits alterations associated with “cellular responses to stress”, which include changes in proteins involved in translation, mitochondrial metabolism, cytoskeleton remodeling, cellular senescence and apoptosis (**fig. 4B and table S2**). Consistent with these changes, *ex vivo* infection of $CD4^+$ T cells resulted in a decrease of 10% in cell viability 24h after infection even with a low MOI (0.1) (**fig. S10C**).

The infection of $CD4^+$ T cells by HIV also causes an increase in IL-10 production[28,29]. The expression and release of IL-10 has been widely associated with chronic viral infections and determines viral persistence [30]. Noteworthy, increased serum levels of IL-10 are associated with COVID-19 severity[31,32]. We found that *IL10* expression by $CD4^+$ T cells was higher in BAL (**fig. S10B**) and blood (**fig. 4C**) of severe COVID-19 patients. These changes were at least in part cell autonomous, since purified $CD4^+$ T cells infected *ex vivo* with SARS-CoV-2 also expressed higher levels of *IL10* (**fig. S10D**). Due to the immunomodulatory role of IL-10, we measured the expression of key pro- and anti-inflammatory cytokines involved in the immune response elicited by $CD4^+$ T cells. $CD4^+$ T cells from severe COVID-19 patients presented decreased expression of *IFNG* and *IL17A* in relation to cells from patients with the moderate form of the disease or healthy donors (**fig. 4C**). These results show that SARS-CoV-2 infection induces *IL10* expression in $CD4^+$ T cells. This phenomenon is associated with a suppression of genes that encode key pro-inflammatory cytokines produced by $CD4^+$ T cells, such as IFNγ and IL-17A, and correlates with disease severity.

Upregulation of *IL10* in HIV-infected cells requires STAT3-independent activation of the transcription factor CREB-1 via Ser^{133} phosphorylation[33]**.** Consistent with the similarities between SARS-CoV-2 and HIV infections, CREB-1 phosphorylation at Ser^{133} was increased in SARS-CoV-2-infected $CD4^+$ T cells (**fig. 4D and S10E**). Thus, SARS-CoV-2 infection appears to directly trigger a signaling cascade that culminates in upregulation of *IL10* in $CD4^+$ T cells. Indeed, expression of *IL10* is positively correlated with viral load in circulating $CD4^+$ T cells from COVID-19 patients (**fig. 4E**). Altogether, our data demonstrate that SARS-CoV-2 infects $CD4^+$ T cells, impairs cell function, leads to increased *IL10* expression and compromises cell viability, which in turn dampens immunity against the virus and contributes to disease severity.

Impaired innate and adaptive immunity is a hallmark of COVID-19, particularly in patients who progress to the critical stages of the disease[34,35]. Here we show that the alterations in immune response associated with the severe illness from COVID-19 are triggered by infection of $CD4^+$ T helper cells by SARS-CoV-2 and consequent dysregulation of immune function.

T helper cells are infected by SARS-CoV-2 using a mechanism that involves binding of sCoV-2 to CD4 and entry via the canonical ACE2/TMPRSS2 pathway. Our model suggests the hypothesis that CD4 stabilizes SARS-CoV-2 on the cell membrane until the virus encounters an ACE2 molecule to enter the cell (**fig. S11**). This mechanism is similar to what has been described for HIV infection. Once in $CD4^+$ T cells, SARS-CoV-2 leads to protein expression changes consistent with alterations in pathways related to stress response, apoptosis and cell cycle regulation which, if sustained, culminate in cell dysfunction and may lead to cell death. SARS-CoV-2 infection also results in phosphorylation of CREB-1 transcription factor and induction of its target gene *IL10* in a cell autonomous manner. Yet again, this mechanism resembles HIV infection[33]**.**.

IL-10 is a powerful anti-inflammatory cytokine and has been previously associated with viral persistence [30]. Serum levels of IL-10 increase during the early stages of the disease – when viral load reaches its peak – and may predict COVID-19 outcome[31,32]. This increase occurs only in patients with the severe form of COVID-19[32]. Consistent with these findings, we found that expression of *IL10* positively correlates with viral load in $CD4^+$ T cells. This is an unique feature of patients with the severe form of COVID-19, since we could not detect the virus in $CD4^+$ T cells from patients with the moderate form of the disease and *IL10* expression in $CD4^+$ T cells is much lower in these patients. In contrast, we found *IFNG* and *IL17A* to be upregulated in $CD4^+$ T cells of patients with the moderate illness, indicating a protective role for these cytokines. However, in patients with the severe symptoms, the expression of *IFNG* and *IL17A* in $CD4^+$ T cells is dampened. IL-10 is a known suppressor of Th1 and Th17

responses[36] and it is likely to contribute to the changes in *IFNG* and *IL17A.* These features will ultimately reflect in the quality of the immune response, which in combination with T cell death and consequent lymphopenia, may result in transient/acute immunodeficiency and impair adaptive immunity in severe COVID-19 patients[6-8].

How long these alterations in T cell function persist *in vivo* and whether they have long-lasting impacts on adaptive immunity remains to be determined. Hence, avoiding T cell infection by blocking sCoV-2-CD4 interaction and boosting T cell resistance against SARS-CoV-2 might represent complementary therapeutic approaches to preserve immune response integrity and prevent patients from progressing to the severe stages of COVID-19.

Author Contributions

A.S.F., G.G.D., A.C.C., N.S.B., V.O.B., L.B.M., T.L.K., J.V.V-LS, R.G.L., P.B.R. and A.B.S.P.G. performed most of the experimental work. B.G.C., A.B.P., L.D.C., M.C. and R.E.M. performed electron microscopy data collection. G.S.P., N.S.W. and J.A.G. performed co-immunoprecipitation assay and immunoblotting. L.N.S., L.I.B. and H.M-S. performed *in situ* hybridization and immunofluorescence analysis. V.C.S., E.B.O. and V.M.F. designed and produced ACE2 blocking peptide. V.C.C., L.C.S-C., F.C. and D.M-S. performed proteomic analyses. D.M., R.F.C., I.C. and H.I.N. performed bioinformatic analyses. A.J.R.F., A.H.S.D., G.L. and M.S. performed docking and molecular modeling analyses. A.P., E.M., R.G.U., A.F.B., T.A.N., L.C.R., M.V.A., M.L.M., H.R.C., FBP, A.C.S., R.S.C. and L.A.V. selected and recruited COVID-19 patients and healthy donors. A.C.C., G.F.S, S.P.M., J.F.M.R.A., D.A.T.T., P.L.P., M.C.M., K.B-S., C.L.S., F.G. and J.L.P.M. conducted the experiments with SARS-CoV-2 in the BSL-3 facility. A.S.F., M.A.M., P.M.M-V., D.M-S., M.S., L.M.B.S., M.A.R.V., A.S.V., A.D., L.A.V., R.E.M., J.L.P.M., H.M-S. and H.I.N. directed parts of the study and provide reagents. A.S.F. and M.A.M. coordinated the study and wrote the manuscript with inputs from all of the co-authors.

Financial Support

This work was supported by grants from FAEPEX-UNICAMP (#2295/20, #2458/20, #2266/20 and #2274/20), São Paulo Research Foundation (FAPESP) (#2019/16116-4, #2019/06372-3, #2020/04583-4, #2013/08293-7, #2020/04579-7, #2015/15626-8, #2018/14933-2, #2020/04746-0, #2019/00098-7, #2020/04919-2, #2017/01184-9), the National Institute of Science and Technology in Neuroimmunomodulation (INCT-NIM) (#465489/2014-1) and FINEP (#01.20.0003.00). A.S.F. and M.A.M. were supported by CNPq productivity awards (#306248/2017-4 and #310287/2018-9). A.J.R.F, G.G.D., A.C.C., N.S.B., L.B.M., F.C., V.C.C., A.B., T.L.K, G.S.P., R.G.L. were supported by FAPESP fellowships (#2019/17007-4, #2019/22398-2, #2019/05155-9, #2019/06459-1, #2019/04726-2, #2017/23920-9, #2016/24163-4, #2016/23328-0). V.O.B. and L.N.S. were supported by FAEPEX fellowship (#2295/20 and #2319/20). D.M. was supported by CAPES fellowship.

Acknowledgment

The authors acknowledge the technical support of Elzira E. Saviani, Paulo A. Baldasso and Mariana Ozello Baratti. The authors would like to thank Dr. Leda Castilho (UFRJ), for providing

sCoV-2 recombinant protein and Dr. Hernandes F. de Carvalho (UNICAMP), for providing valuable reagents for ICC. We thank the National Institute of Science and Technology of Photonics Applied to Cell Biology (INFABIC) for aid with confocal microscopy.

References

1. Zhang, X. *et al.* Viral and host factors related to the clinical outcome of COVID-19. *Nature* **583,** 437–440 (2020).
2. Laing, A. G. *et al.* A dynamic COVID-19 immune signature includes associations with poor prognosis. *Nat. Med.* **579,** 1–13 (2020).
3. Li, R. *et al.* Substantial undocumented infection facilitates the rapid dissemination of novel coronavirus (SARS-CoV-2). *Science* **368,** 489–493 (2020).
4. Candido, D. S. *et al.* Evolution and epidemic spread of SARS-CoV-2 in Brazil. *Science* eabd2161 (2020). doi:10.1126/science.abd2161
5. Moore, J. B. & June, C. H. Cytokine release syndrome in severe COVID-19. *Science* **368,** 473–474 (2020).
6. Thoms, M. *et al.* Structural basis for translational shutdown and immune evasion by the Nsp1 protein of SARS-CoV-2. *Science* **12,** eabc8665 (2020).
7. De Biasi, S. *et al.* Marked T cell activation, senescence, exhaustion and skewing towards TH17 in patients with COVID-19 pneumonia. *Nat Comms* **11,** 1–17 (2020).
8. Arunachalam, P. S. *et al.* Systems biological assessment of immunity to mild versus severe COVID-19 infection in humans. *Science* eabc6261 (2020). doi:10.1126/science.abc6261
9. Robbiani, D. F. *et al.* Convergent antibody responses to SARS-CoV-2 in convalescent individuals. *Nature* 1–8 (2020). doi:10.1038/s41586-020-2456-9
10. Long, Q.-X. *et al.* Clinical and immunological assessment of asymptomatic SARS-CoV-2 infections. *Nat. Med.* **63,** 1–5 (2020).
11. Hoffmann, M. *et al.* SARS-CoV-2 Cell Entry Depends on ACE2 and TMPRSS2 and Is Blocked by a Clinically Proven Protease Inhibitor. *Cell* **181,** 271–280.e8 (2020).
12. Lamers, M. M. *et al.* SARS-CoV-2 productively infects human gut enterocytes. *Science* **369,** 50–54 (2020).
13. Codo, A. C. *et al.* Title: Elevated glucose levels favor SARS-CoV-2 infection and monocyte response through a HIF-1α/glycolysis dependent axis. *Cell Metabolism* (2020). doi:10.1016/j.cmet.2020.07.007
14. Yang, L. *et al.* A Human Pluripotent Stem Cell-based Platform to Study SARS-CoV-2 Tropism and Model Virus Infection in Human Cells and Organoids. *Cell Stem Cell* **27,** 125–136.e7 (2020).
15. Wrapp, D. *et al.* Cryo-EM structure of the 2019-nCoV spike in the prefusion conformation. *Science* **367,** 1260–1263 (2020).
16. Yuan, M. *et al.* A highly conserved cryptic epitope in the receptor binding domains of SARS-CoV-2 and SARS-CoV. *Science* **368,** 630–633 (2020).
17. Lasso, G. *et al.* A Structure-Informed Atlas of Human-Virus Interactions. *Cell* **178,** 1526–+ (2019).
18. Shaik, M. M. *et al.* Structural basis of coreceptor recognition by HIV-1 envelope spike. *Nature* **565,** 318–323 (2019).
19. O'Shea, J. J. & Paul, W. E. Mechanisms Underlying Lineage Commitment and Plasticity of Helper CD4+ T Cells. *Science* **327,** 1098–1102 (2010).
20. Gasteiger, G. & Rudensky, A. Y. Interactions between innate and adaptive lymphocytes. *Nat Rev Immunol* **14,** 631–639 (2014).
21. Xu, X.-N., Screaton, G. R. & McMichael, A. J. Virus Infections: Escape, Resistance, and Counterattack. *Immunity* **15,** 867–870 (2001).
22. Liao, M. *et al.* Single-cell landscape of bronchoalveolar immune cells in patients with COVID-19. *Nat. Med.* **19,** 1–3 (2020).
23. Hioe, C. E. *et al.* Inhibition of Human Immunodeficiency Virus Type 1 gp120 Presentation to CD4 T Cells by Antibodies Specific for the CD4 Binding Domain of gp120. *J. Virol.* **75,** 10950–10957 (2001).

24. Wang, H. *et al.* Cryo-EM structure of a CD4-bound open HIV-1 envelope trimer reveals structural rearrangements of the gp120 V1V2 loop. *Proc. Natl. Acad. Sci. U.S.A.* **113,** E7151–E7158 (2016).
25. Iliopoulou, M. *et al.* A dynamic three-step mechanism drives the HIV-1 pre-fusion reaction. *Nat Struct Mol Biol* **25,** 814–822 (2018).
26. Lee, J. H., Ozorowski, G. & Ward, A. B. Cryo-EM structure of a native, fully glycosylated, cleaved HIV-1 envelope trimer. *Science* **351,** 1043–1048 (2016).
27. Golumbeanu, M. *et al.* Proteo-Transcriptomic Dynamics of Cellular Response to HIV-1 Infection. *Sci Rep* **9,** 1–12 (2019).
28. Doitsh, G. *et al.* Cell death by pyroptosis drives CD4 T-cell depletion in HIV-1 infection. *Nature* **505,** 509–514 (2013).
29. Brockman, M. A. *et al.* IL-10 is up-regulated in multiple cell types during viremic HIV infection and reversibly inhibits virus-specific T cells. *Blood* **114,** 346–356 (2009).
30. Brooks, D. G. *et al.* Interleukin-10 determines viral clearance or persistence in vivo. *Nat. Med.* **12,** 1301–1309 (2006).
31. Han, H. *et al.* Profiling serum cytokines in COVID-19 patients reveals IL-6 and IL-10 are disease severity predictors. *Emerging Microbes & Infections* **9,** 1123–1130 (2020).
32. Zhao, Y. *et al.* Longitudinal COVID-19 profiling associates IL-1RA and IL-10 with disease severity and RANTES with mild disease. *J. Clin. Invest.* **5,** (2020).
33. Gee, K. *et al.* Intracellular HIV-Tat Expression Induces IL-10 Synthesis by the CREB-1 Transcription Factor through Ser 133Phosphorylation and Its Regulation by the ERK1/2 MAPK in Human Monocytic Cells. *J. Biol. Chem.* **281,** 31647–31658 (2006).
34. Hadjadj, J. *et al.* Impaired type I interferon activity and inflammatory responses in severe COVID-19 patients. *Science* **369,** 718–724 (2020).
35. Mathew, D. *et al.* Deep immune profiling of COVID-19 patients reveals distinct immunotypes with therapeutic implications. *Science* eabc8511 (2020). doi:10.1126/science.abc8511
36. Wilson, E. B. & Brooks, D. G. in *Negative Co-Receptors and Ligands* (eds. Ahmed, R. & Honjo, T.) **350,** 39–65 (Springer Berlin Heidelberg, 2010).

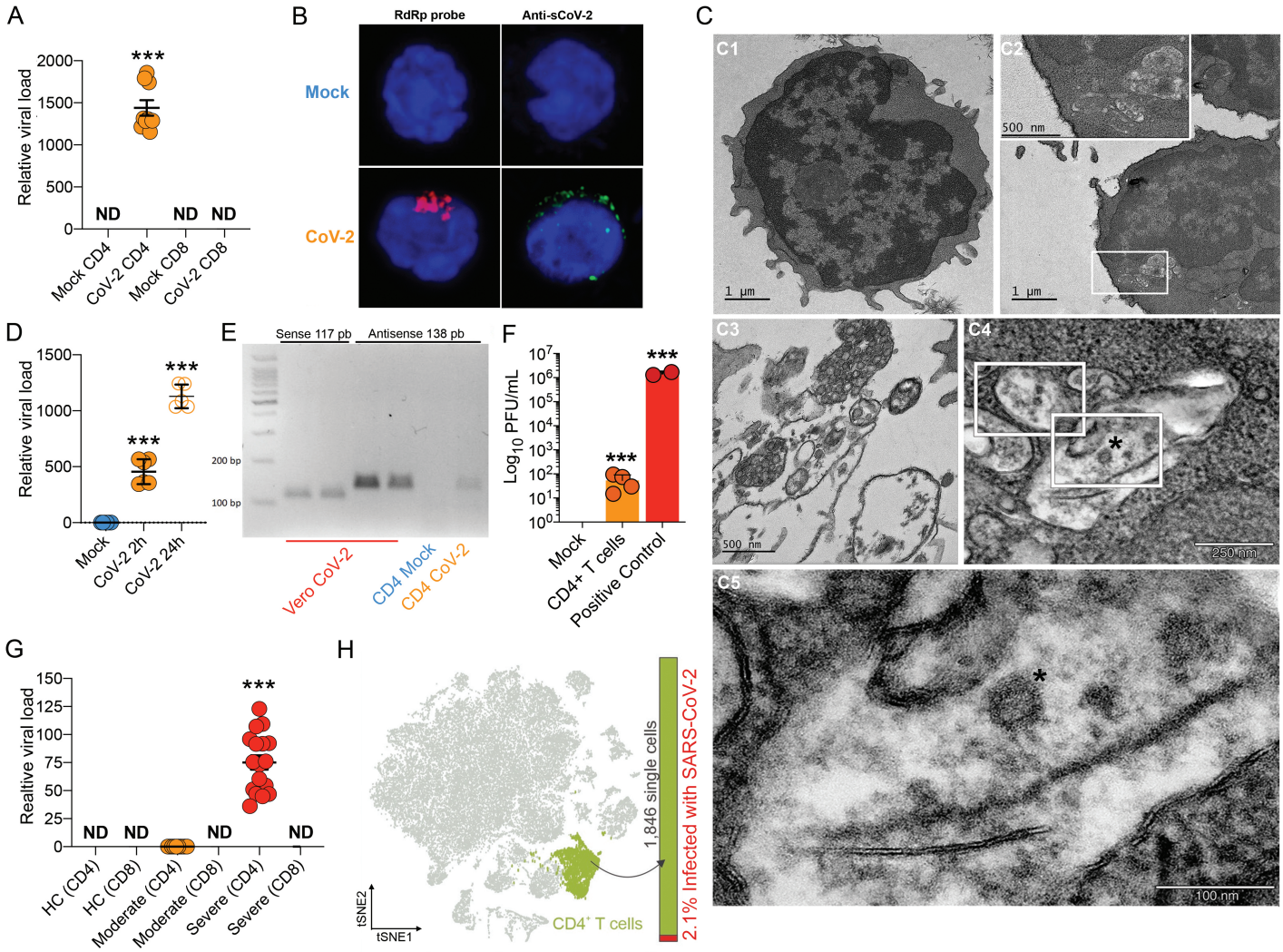
A
Relative viral load
2000
1500
1000
500
0
***
ND
ND
ND
Mock CD4
CoV-2 CD4
Mock CD8
CoV-2 CD8
B
RdRp probe
Anti-sCoV-2
Mock
CoV-2
C
C1
1 µm
C2
500 nm
1 µm
C3
500 nm
C4
250 nm
C5
100 nm
D
Relative viral load
1500
1000
500
0
***
***
Mock
CoV-2 2h
CoV-2 24h
E
Sense 117 pb
Antisense 138 pb
200 bp
100 bp
Vero CoV-2
CD4 Mock
CD4 CoV-2
F
Log10 PFU/mL
***
***
Mock
CD4+ T cells
Positive Control
G
Realtive viral load
150
125
100
75
50
25
0
***
ND
ND
ND
ND
HC (CD4)
HC (CD8)
Moderate (CD4)
Moderate (CD8)
Severe (CD4)
Severe (CD8)
H
tSNE2
tSNE1
CD4+ T cells
1,846 single cells
2.1% Infected with SARS-CoV-2

Figure 1

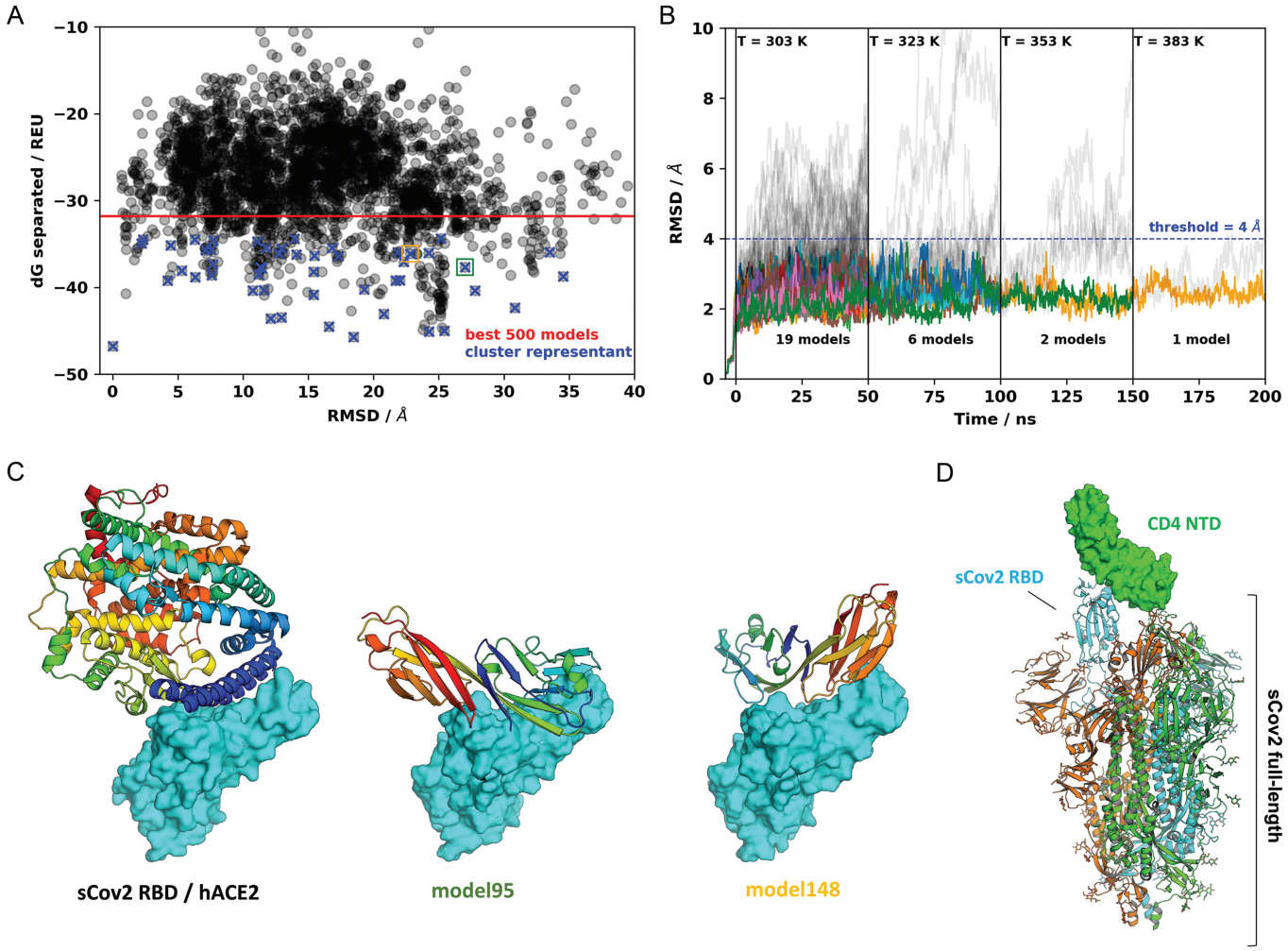
A
dG separated / REU
RMSD / Å
best 500 models
cluster representant
B
RMSD / Å
Time / ns
T = 303 K
T = 323 K
T = 353 K
T = 383 K
threshold = 4 Å
19 models
6 models
2 models
1 model
C
sCov2 RBD / hACE2
model95
model148
D
CD4 NTD
sCov2 RBD
sCov2 full-length

Figure 2

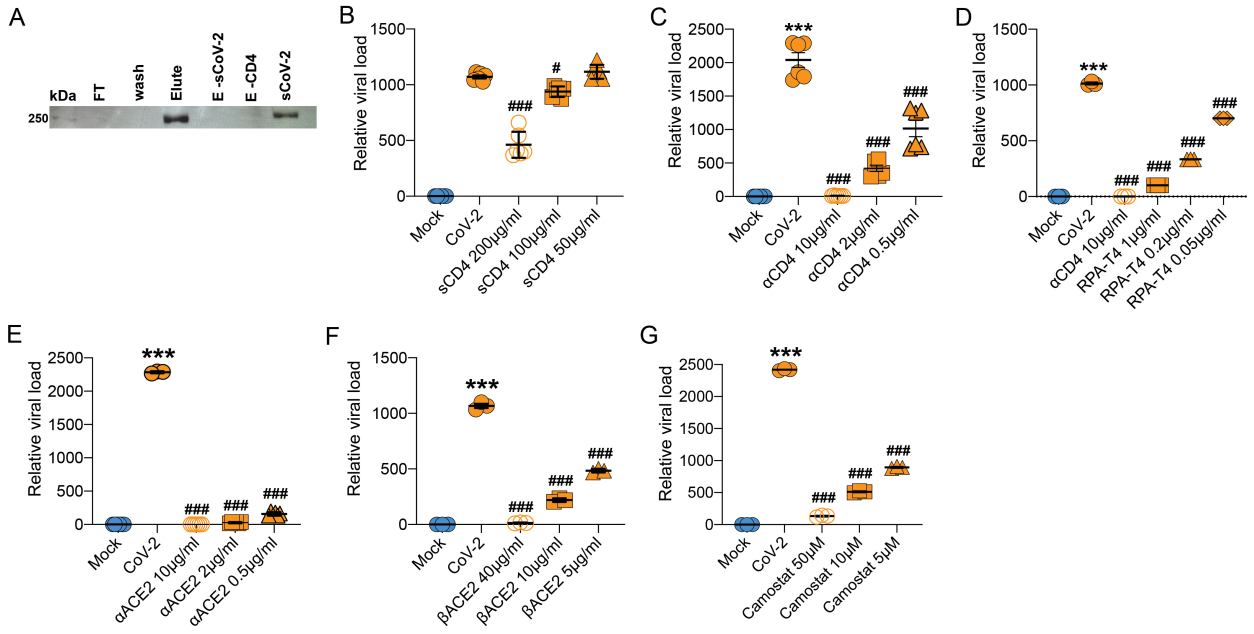
A
kDa
FT
wash
Elute
E -sCoV-2
E -CD4
sCoV-2
250
B
Relative viral load
Mock
CoV-2
sCD4 200μg/ml
sCD4 100μg/ml
sCD4 50μg/ml
C
αCD4 10μg/ml
αCD4 2μg/ml
αCD4 0.5μg/ml
D
RPA-T4 1μg/ml
RPA-T4 0.2μg/ml
RPA-T4 0.05μg/ml
E
αACE2 10μg/ml
αACE2 2μg/ml
αACE2 0.5μg/ml
F
βACE2 40μg/ml
βACE2 10μg/ml
βACE2 5μg/ml
G
Camostat 50μM
Camostat 10μM
Camostat 5μM

Figure 3

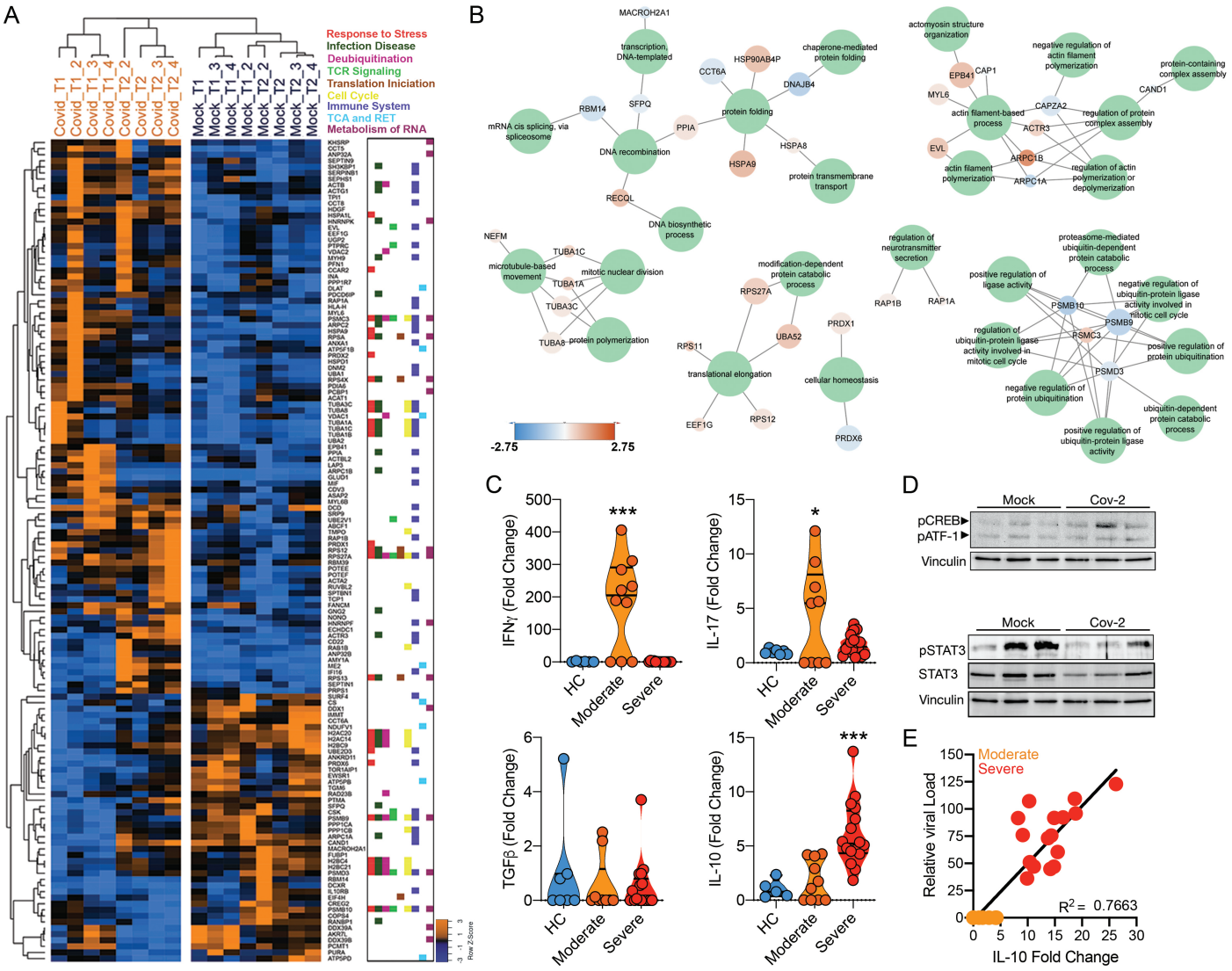
A
Covid_T1
Covid_T1_2
Covid_T1_3
Covid_T1_4
Covid_T2_2
Covid_T2
Covid_T2_3
Covid_T2_4
Mock_T1
Mock_T1_3
Mock_T1_4
Mock_T1_2
Mock_T2_2
Mock_T2
Mock_T2_3
Mock_T2_4
Response to Stress
Infection Disease
Deubiquitination
TCR Signaling
Translation Iniciation
Cell Cycle
Immune System
TCA and RET
Metabolism of RNA
Row Z-Score
B
MACROH2A1
transcription, DNA-templated
SFPQ
RBM14
mRNA cis splicing, via spliceosome
DNA recombination
RECQL
DNA biosynthetic process
CCT6A
HSP90AB4P
chaperone-mediated protein folding
DNAJB4
protein folding
PPIA
HSPA8
HSPA9
protein transmembrane transport
actomyosin structure organization
negative regulation of actin filament polymerization
protein-containing complex assembly
CAND1
EPB41
CAP1
MYL6
actin filament-based process
CAPZA2
ACTR3
regulation of protein complex assembly
EVL
ARPC1B
actin filament polymerization
ARPC1A
regulation of actin polymerization or depolymerization
NEFM
TUBA1C
microtubule-based movement
mitotic nuclear division
TUBA1A
TUBA3C
TUBA8
protein polymerization
modification-dependent protein catabolic process
RPS27A
UBA52
PRDX1
RPS11
translational elongation
cellular homeostasis
EEF1G
RPS12
PRDX6
regulation of neurotransmitter secretion
RAP1B
RAP1A
proteasome-mediated ubiquitin-dependent protein catabolic process
positive regulation of ligase activity
negative regulation of ubiquitin-protein ligase activity involved in mitotic cell cycle
PSMB10
PSMB9
PSMC3
regulation of ubiquitin-protein ligase activity involved in mitotic cell cycle
positive regulation of protein ubiquitination
PSMD3
negative regulation of protein ubiquitination
ubiquitin-dependent protein catabolic process
positive regulation of ubiquitin-protein ligase activity
-2.75
2.75
C
IFNγ (Fold Change)
IL-17 (Fold Change)
TGFβ (Fold Change)
IL-10 (Fold Change)
HC
Moderate
Severe
***
*
D
Mock
Cov-2
pCREB
pATF-1
Vinculin
pSTAT3
STAT3
E
Moderate
Severe
Relative viral Load
IL-10 Fold Change
R^2 = 0.7663

Figure 4

Legends

Figure 1. SARS-CoV-2 infects CD4$^+$ T cells *in vitro* and *in vivo*

Peripheral blood CD3$^+$CD4$^+$ and CD3$^+$CD8$^+$ were infected with mock control or SARS-CoV-2 (CoV-2) (MOI 0.1) for 1 h under continuous agitation. **(A)** Viral load was assessed by RT-qPCR 24 h after infection. **(B)** Cells were washed, cultured for 24 h, fixed with PFA 4% and stained with RdRp probe for *in situ* hybridization or anti-sCoV-2 for immunofluorescence. Cells were analyzed by confocal microscopy. **(C) C1-C5** - Representative transmission electron microscopy (EM) micrographs showing viral particles (asterisks) inside lymphocytes 2 h after infection. **(D)** Viral load was determined by qPCR 2 h and 24 h after infection. **(E)** PCR for antisense CoV-2 strand was performed in CD4$^+$ T and Vero (positive control) cells infected with mock or CoV-2. **(F)** Vero cells were incubated with the supernatant of mock control or CoV-2 infected CD4$^+$ T cells under continuous agitation for 1 h. The viral load in Vero cells was measured after 72 h using plaque assay. PFU – plaque-forming unit. **(G)** Viral load was measured by RT-qPCR in peripheral blood CD4$^+$ and CD8$^+$ T cells from healthy controls (HC), moderate and severe COVID-19 patients. **(H)** CoV-2 RNA detection in CD4$^+$ T cells from bronchoalveolar lavage (BAL) single-cell sequencing data revealing the presence of CoV-2 RNA. Data represent mean ± SEM of at least two independent experiments performed in triplicate or duplicate (f). ***$p < 0.001$ compared to all. ND=not detected.

Figure 2. A model for sCoV-2 RBD and CD4 NTD interaction.

(A) Interaction energy (dG separated) versus RMSD plot shows a high diversity of binding modes with similar energies. Among the 500 best models, 50 cluster best ranked representatives (shown as blue crosses) were selected for further evaluation with molecular dynamics simulations. **(B).** RMSD to the initial docked complex as a function of molecular dynamics simulation time over 200 ns and four steps of temperature. At each temperature step, well behaved models are depicted as colored curves, while divergent candidates are shown as grey curves. Kinetically stable models making reasonable interactions remain close to their initial docked conformation. Only two models remain stable after the third step of 50 ns at 353K. For both models, resilient contacts throughout simulation are shown in Fig. S5. **(C)** Interaction models of ACE2 and sCoV-2 RBD. The two best candidates according to molecular dynamics simulation, model95 and model148, present distinct binding modes. For the first case, interaction occurs mainly in the N-terminal portion of CD4 NTD, while the latter have important contributions of the central part of this domain. **(D)** Full-length model of sCoV-

2 and CD4 NTD interaction obtained by alignment of sCoV-2 RBD from model 148 to the sCoV-2 RBD opened state from PDB 6vyb EM structure.

Figure 3. Infection of CD4$^+$ T cell by SARS-CoV-2 is dependent on CD4 and ACE2 molecules.

(A) Recombinant sCoV-2 (with twin-strep-tag) and CD4 were co-incubated and immunoprecipitated with anti-CD4. Complex formation was determined by affinity blotting using streptavidin-HRP. **(B)** Cells were infected with mock control or SARS-CoV-2 (CoV-2) in the presence of vehicle or soluble CD4 (sCD4) in different concentrations (200, 100 or 50 µg/ml) for 1h under continuous agitation. Viral load was assessed by RT-qPCR 24 h after infection. **(C-D).** Primary human CD4$^+$ T cells were stimulated with IgG control, or anti-CD4: **(C)** polyclonal (αCD4) or **(D)** monoclonal (RPA-T4) antibody 18 h prior to infection with mock control or CoV-2. Viral load was determined by RT-qPCR 24 h after infection. **(E)** Peripheral blood CD4$^+$ T cells were stimulated with IgG control or anti-ACE2 (αACE2) polyclonal antibody 18 h prior to infection with mock control or CoV-2 for 1 h. Viral load was determined 24 h after infection. **(F)** Human CD4$^+$ T cells were incubated for 1 h prior to infection with control peptide or a peptide that binds to the domain of ACE2 that interacts with sCoV-2 (βACE2). The cells were infected with mock control or CoV-2 for 1 h and viral load analyzed 24 h later by RT-qPCR. **(G)** CD4$^+$ T cells were incubated with vehicle or camostat mesylate for 18 h before the infection with mock control or CoV-2 for 1h. Viral load was analyzed by RT-qPCR. Data represent mean ± SEM of at least two independent experiments performed in triplicate. ***$p < 0.0001$ compared to all; $^{###}p < 0.001$, $^{\#}$ $p < 0.05$ compared to CoV-2

Figure 4. Infection of CD4$^+$ T cells by SARS-CoV-2 alters cell function and triggers IL-10 production

(A) Heatmap of differentially expressed proteins and their associated biological processes. **(B)** Network of differentially expressed proteins and their associated biochemical pathways. **(C)** Relative expression of *IFNG, IL17, TGFB1,* and *IL10* in peripheral blood CD3$^+$CD4$^+$ cells from COVID-19 patients (moderate or severe) and healthy control (HC). Data represent mean ± SEM. Each dot represents a patient sample. (**D**) Representative immunoblotting of CREB-1^{Ser133} and STAT3 in Peripheral blood CD3$^+$CD4$^+$ infected with mock control or SARS-CoV-2.

***$p < 0.001$, **$p < 0.00$, *$p < 0.05$ compared to all.